Ambiguities in the Implementation of the Impulse Approximation for the Response of Many-Fermion Systems

Omar Benhar,[1] Adelchi Fabrocini,[2] and Stefano Fantoni[3]
[1]*INFN, Sezione Roma 1, I-00185 Roma, Italy*
[2]*Department of Physics, University of Pisa, and INFN, I-56100 Pisa, Italy*
[3]*International School for Advanced Studies (SISSA), I-30014 Trieste, Italy*
(Received 8 March 2001; published 11 July 2001)

Within the impulse approximation, the response of a many-body system at large momentum transfer can be directly related to ground state properties. Although the physics assumptions underlying impulse approximation are well defined, their implementation involves ambiguities that may cause significant differences in the calculated responses. We show that, while minimal use of the impulse approximation assumptions naturally leads to write the response in terms of the spectral function, the alternative definition in terms of the momentum distribution involves a more extended use of the same assumptions.

DOI: 10.1103/PhysRevLett.87.052501 PACS numbers: 24.10.Cn, 25.30.Fj, 61.12.Bt

The purpose of this Letter is to show that a truly unambiguous definition of the response of a strongly interacting many-body system to an external probe, within the impulse approximation (IA), must be based on the use of the target spectral function, rather than its momentum distribution.

The main assumption underlying IA is that, as the space resolution of a probe delivering momentum $\mathbf{q}$ to a many-body system is $\sim 1/|\mathbf{q}|$, at large enough $|\mathbf{q}|$ the target is seen by the probe as a collection of individual constituents. Within this picture, the response measures the probability that, after giving one of the constituents a momentum $\mathbf{q}$ at time $t = 0$, the system be reverted to the ground state after time t giving the *same* constituent a momentum $-\mathbf{q}$.

The second assumption involved in IA is that final state interactions (FSI), taking place at $t < t' < 0$ between the hit constituent and the $(N-1)$-particle spectator system, be negligible. The most popular argument supporting this assumption is based on the observation that, compared to the amplitude in the absence of FSI, the amplitude of the process including a rescattering in the final state involves an extra propagator, describing the motion of the struck particle carrying a momentum $\sim\mathbf{q}$. As a consequence, this amplitude is expected to be suppressed when $|\mathbf{q}|$ is large.

In spite of the fact that the two basic assumptions underlying IA can be unambiguously stated, in the literature one finds two different definitions of the IA response, involving either the target spectral function [1] or its momentum distribution [2].

The two different definitions arise from different implementations of the IA assumptions and may lead to significantly different numerical results. In addition, as IA can be seen as the zeroth order of a systematic approximation scheme, to be improved upon including FSI effects, the ambiguity in the IA response poses a serious problem, making it difficult to identify genuine FSI effects. This feature is particularly critical in the analysis of the electromagnetic response of nuclear systems, where FSI are believed to play a relevant role even at large $|\mathbf{q}|$ [3].

In this short Letter we show that the definition of the response in terms of the spectral function follows from minimal use of the assumptions involved in the IA scheme and correctly takes into account the correlation between momentum and removal energy of the hit constituent. On the other hand, a more extended use of the same assumptions leads to the definition in terms of the momentum distribution, which totally disregards the effect of the removal energy distribution.

The response of an N-particle system to a scalar probe is defined as [2]

$$S(\mathbf{q},\omega) = \frac{1}{N}\int \frac{dt}{2\pi}\, e^{i\omega t}\langle 0|\rho_{\mathbf{q}}^{\dagger}(t)\rho_{\mathbf{q}}(0)\,|0\rangle = \frac{1}{N}\int \frac{dt}{2\pi}\, e^{i\omega t}\langle 0|e^{iHt}\rho_{\mathbf{q}}^{\dagger}e^{-iHt}\rho_{\mathbf{q}}|0\rangle\,, \quad (1)$$

where $\mathbf{q}$ and ω denote the momentum and energy transfer, respectively, H and $|0\rangle$ are the target Hamiltonian and ground state, satisfying the Schrödinger equation $H|0\rangle = E_0|0\rangle$, and $\rho_{\mathbf{q}} = \sum_{\mathbf{k}} a^{\dagger}_{\mathbf{k}+\mathbf{q}}a_{\mathbf{k}}$, $a^{\dagger}_{\mathbf{k}+\mathbf{q}}$ and $a_{\mathbf{k}}$ being the usual creation and annihilation operators. Note that the above definition can be readily generalized to describe the electromagnetic response replacing $\rho_{\mathbf{q}}$ with the appropriate electromagnetic current operator.

Using the Schrödinger equation to get rid of one of the propagators appearing in Eq. (1) we obtain

$$S(\mathbf{q},\omega) = \frac{1}{N}\int \frac{dt}{2\pi}\, e^{i(\omega+E_0)t}\langle 0|\rho_{\mathbf{q}}^{\dagger}e^{-iHt}\rho_{\mathbf{q}}|0\rangle\,. \quad (2)$$

The above definition can be simplified introducing the first assumption involved in IA, i.e., that the process involves only one constituent, while the remaining $(N-1)$ particles act as spectators. As a result, the ground state expectation value appearing in Eq. (2) can be rewritten in configuration space as [$R \equiv (\mathbf{r}_1,\ldots,\mathbf{r}_N)$ specifies the positions of the N target constituents]

$$\langle 0|\rho_{\mathbf{q}}^{\dagger} e^{-iHt} \rho_{\mathbf{q}}|0\rangle = N \int dR dR' \, \Psi_0^*(R) e^{-i\mathbf{q}\cdot\mathbf{r}_1} \times \langle R|e^{-iHt}|R'\rangle e^{i\mathbf{q}\cdot\mathbf{r}_1'} \Psi_0(R'), \quad (3)$$

where $\Psi_0(R) = \langle R \,|\, 0\rangle$ is the ground state wave function.

The N-particle Hamiltonian H can be split according to

$$H = H_0 + T_1 + H_{\mathrm{FSI}}, \quad (4)$$

where H_0 denotes the Hamiltonian of the spectator system

$$H_0 = \sum_{i=2}^{N} -\frac{\nabla_i^2}{2m} + \sum_{j>i=2}^{N} v_{ij}, \quad (5)$$

v_{ij} and m being the potential describing the interactions between target constituents and the constituent mass, respectively. The remaining two terms in Eq. (4) are the kinetic energy of the struck particle,

$$T_1 = -\frac{\nabla_1^2}{2m}, \quad (6)$$

and

$$H_{\mathrm{FSI}} = \sum_{j=2}^{N} v_{1j}. \quad (7)$$

The second assumption involved in IA amounts to disregarding the contribution of H_{FSI}, describing the FSI between the hit constituent and the spectators. As H_0 and T_1 obviously commute, this allows one to rewrite the configuration space N-body propagator appearing in Eq. (3) in the simple factorized form [$\tilde{R} \equiv (\mathbf{r}_2 \cdots \mathbf{r}_N)$]

$$\langle R|e^{-iHt}|R'\rangle = \langle \tilde{R}|e^{-iH_0 t}|\tilde{R}'\rangle \langle \mathbf{r}_1|e^{-iT_1 t}|\mathbf{r}_1'\rangle. \quad (8)$$

The two propagators on the right-hand side (rhs) of the above equation can be written in spectral representation as

$$\langle \tilde{R}|e^{-i\mathrm{H}_0 t}|\tilde{R}'\rangle = \sum_n e^{-iE_n t} \Phi_n(\tilde{R}) \Phi_n^*(\tilde{R}') \quad (9)$$

and

$$\langle \mathbf{r}_1|e^{-iT_1 t}|\mathbf{r}_1'\rangle = \int \frac{d^3p}{(2\pi)^3} e^{-iE_p t} e^{i\mathbf{p}\cdot(\mathbf{r}_1 - \mathbf{r}_1')}, \quad (10)$$

where $\Phi_n(\tilde{R}) = \langle \tilde{R} \,|\, n\rangle$, E_n and $|n\rangle$ satisfy the $(N-1)$-particle Schrödinger equation $H_0|n\rangle = E_n|n\rangle$, and $E_p = \mathbf{p}^2/2m$.

Using Eqs. (9) and (10) and substituting Eq. (8) into Eq. (3) we get

$$\langle 0|\rho_{\mathbf{q}}^{\dagger} e^{-iHt} \rho_{\mathbf{q}}|0\rangle = N \int \frac{d^3p}{(2\pi)^3} \sum_n e^{-i(E_p + E_n)t} \times \left| \int dR \, e^{i(\mathbf{p}-\mathbf{q})\cdot\mathbf{r}_1} \Psi_0^*(R) \Phi_n(\tilde{R}) \right|^2. \quad (11)$$

Finally, substitution of the above result into Eq. (2) leads to

$$S(\mathbf{q}, \omega) = \int \frac{d^3p}{(2\pi)^3} dE \, P(\mathbf{p} - \mathbf{q}, E) \delta(\omega - E_p - E), \quad (12)$$

where the spectral function, defined as

$$P(\mathbf{k}, E) = \sum_n \left| \int dR \, e^{i\mathbf{k}\cdot\mathbf{r}_1} \Psi_0^*(R) \Phi_n(\tilde{R}) \right|^2 \times \delta(E + E_0 - E_n), \quad (13)$$

measures the probability of removing a constituent of momentum $\mathbf{k}$ from the target ground state leaving the residual system with excitation energy E.

Let us now consider a different way of implementing the physical assumptions underlying IA in the calculation of $S(\mathbf{q}, \omega)$. In going from Eq. (1) to Eq. (2) we have exploited the Schrödinger equation to get rid of one of the two N-body propagators. We have then used the assumption $H_{\mathrm{FSI}} = 0$ to rewrite the remaining propagator in the factorized form that led to the emergence of the spectral function in the formalism. In principle, as IA provides a prescription to rewrite the N-particle propagator in a simpler form, one may just as well use this prescription and rewrite *both* propagators appearing in Eq. (1), rather than use the Schrödinger equation. However, this procedure results in a definition of $S(\mathbf{q}, \omega)$ in which the information on the target removal energy distribution is totally lost.

The ground state expectation value relevant in this case,

$$\langle 0|e^{iHt} \rho_{\mathbf{q}}^{\dagger} e^{-iHt} \rho_{\mathbf{q}}|0\rangle = N \int dR dR' dR'' \, \Psi_0^*(R) \times \langle R|e^{iHt}|R''\rangle e^{-i\mathbf{q}\cdot\mathbf{r}_1''} \times \langle R''|e^{-iHt}|R'\rangle e^{i\mathbf{q}\cdot\mathbf{r}_1'} \Psi_0(R'), \quad (14)$$

can be rewritten using again factorization and the spectral representation. In addition, the dependence upon the state of the spectator system can be removed applying the orthonormality relations

$$\int d\tilde{R} \Phi_n^*(\tilde{R}) \Phi_m(\tilde{R}) = \delta_{nm} \quad (15)$$

and

$$\sum_n \Phi_n^*(\tilde{R}) \Phi_n(\tilde{R}') = \delta(\tilde{R} - \tilde{R}'). \quad (16)$$

As a result, the rhs of Eq. (14) becomes

$$N \int dR \, d^3r_1' \, d^3r_1'' \int \frac{d^3k}{(2\pi)^3} \frac{d^3p}{(2\pi)^3} e^{i(E_k - E_p)t} \Psi_0^*(\mathbf{r}_1, \tilde{R}) e^{i[\mathbf{p} - (\mathbf{k}+\mathbf{q})]\cdot\mathbf{r}_1''} e^{i\mathbf{k}\cdot\mathbf{r}_1} e^{-i(\mathbf{p}-\mathbf{q})\cdot\mathbf{r}_1'} \Psi_0(\mathbf{r}_1', \tilde{R}), \quad (17)$$

and integration over $\mathbf{r}''$ and $\mathbf{p}$ yields

$$\langle 0|e^{iHt}\rho_{\mathbf{q}}^{\dagger}e^{-iHt}\rho_{\mathbf{q}}|0\rangle = N\int \frac{d^3k}{(2\pi)^3}\, e^{i(E_k - E_{|\mathbf{k}+\mathbf{q}|})t} \times \int d^3r_1 d^3r_1'\, e^{i\mathbf{k}\cdot(\mathbf{r}_1-\mathbf{r}_1')} \times \int d\tilde{R}\Psi_0^*(\mathbf{r}_1,\tilde{R})\Psi_0(\mathbf{r}_1',\tilde{R})\,. \quad (18)$$

Finally, substitution of the above equation into Eq. (1) leads to

$$S(\mathbf{q},\omega) = \int \frac{d^3k}{(2\pi)^3}\, n(\mathbf{k})\,\delta(\omega + E_k - E_{|\mathbf{k}+\mathbf{q}|}), \quad (19)$$

where the momentum distribution $n(\mathbf{k})$, yielding the probability to find a constituent carrying momentum $\mathbf{k}$ in the target ground state, is given by

$$n(\mathbf{k}) = \int d^3r_1 d^3r_1'\, e^{i\mathbf{k}\cdot(\mathbf{r}_1-\mathbf{r}_1')} \int d\tilde{R}\Psi_0^*(\mathbf{r}_1,\tilde{R})\Psi_0(\mathbf{r}_1',\tilde{R})\,. \quad (20)$$

Comparison between the above equation and Eq. (13) shows that the momentum distribution is simply related to the spectral function through

$$n(\mathbf{k}) = \int dE\, P(\mathbf{k},E)\,. \quad (21)$$

As a first example, illustrative of the differences between $S(\mathbf{q},\omega)$ evaluated using Eq. (12) and that resulting from Eq. (19), we discuss the response of infinite nuclear matter at equilibrium density $\rho = 0.16$ fm^{-3}.

An *ab initio* microscopic calculation of the nuclear matter spectral function, carried out within the framework of correlated basis function perturbation theory using a realistic Hamiltonian, is described in Ref. [1]. The main feature of the spectral function of Ref. [1] is the presence of a substantial amount of strength at large E, leading to an average removal energy $\bar{\epsilon} = \langle E\rangle = 61.9$ MeV, much larger than the Fermi energy $\epsilon_F = 16$ MeV. In addition, the calculated $P(\mathbf{k},E)$ exhibits a strong correlation between momentum and removal energy, implying that large momentum ($|\mathbf{k}| \gg k_F$, $k_F = 1.33$ fm^{-1} being the Fermi momentum) always corresponds to large removal energy ($E \gg \epsilon_F$). For example, 50% of the strength at $|\mathbf{k}| = 3$ fm^{-1} resides at $E > 200$ MeV [1].

The solid and dashed lines in Fig. 1 show the ω dependence of $S(\mathbf{q},\omega)$ evaluated from Eqs. (12) and (19), respectively, at $|\mathbf{q}| = 5$ fm^{-1}. At this momentum transfer, the nuclear response exhibits scaling in the variable y [4], reflecting the onset of the IA regime [5].

The solid line in Fig. 1 has been obtained using the spectral function of Ref. [1], whereas the momentum distribution employed to obtain the dashed line has been consistently calculated by E integration of the same $P(\mathbf{k},E)$, according to Eq. (21).

While the two curves have similar shape, their width being dictated by the momentum distribution, they appear to be shifted with respect to one another. The peak of the dashed curve is located at energy $\omega \sim |\mathbf{q}|^2/2m_N$, corresponding to elastic scattering off a free stationary nucleon, whereas the solid line, due to the removal energy distribution described by the spectral function, peaks at significantly larger energy. To illustrate this feature we show by diamonds the results obtained replacing E_k with $E_k + \bar{\epsilon}$ in the argument of the energy conserving δ function of Eq. (19). The corresponding response, shifted by $\bar{\epsilon} = 61.9$ MeV with respect to the dashed curve, turns out to be very close to that obtained from Eq. (12).

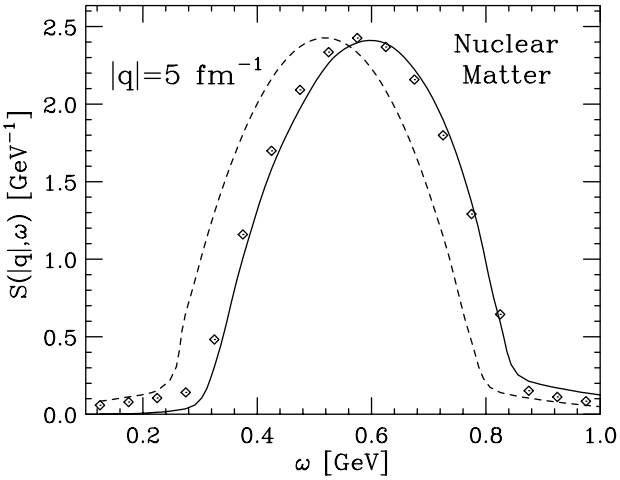

FIG. 1. Infinite nuclear matter $S(|\mathbf{q}|,\omega)$ at equilibrium density and $|\mathbf{q}| = 5$ fm^{-1}. The solid and dashed lines have been obtained from Eqs. (12) and (19), respectively. The diamonds represent the results obtained replacing E_k with $E_k + \bar{\epsilon}$ in the argument of the energy-conserving δ function of Eq. (19).

In addition to the shift in the position of the peak, the dashed and solid lines sizably differ at low energy transfer, where the response obtained using the momentum distribution is much larger than that obtained from Eq. (12). The difference between the two curves in the low ω region makes it difficult to identify corrections to the response of Eq. (19) arising from mechanisms not included in the definition of IA. For example, a quantitative study of FSI effects, which are known to dominate the nuclear response at low ω, should be carried out starting from $S(\mathbf{q},\omega)$ defined as in Eq. (12).

In conclusion, the results of Fig. 1 clearly show that the nuclear responses extracted from electron-nucleus scattering data at momentum transfer in the few GeV/c range (1 GeV/$c \sim 5$ fm^{-1}) must be analyzed using spectral functions according to Eqs. (12) and (13), as in Refs. [3,6].

On the other hand, the definition of $S(\mathbf{q},\omega)$ in terms of the momentum distribution has been successfully used to describe the response of liquid helium, measured by inclusive scattering of thermal neutrons [2,7]. The excellent agreement between the response calculated from Eq. (19) and the experimental one can be explained noting that (i) the region of momentum transfer covered by neutron

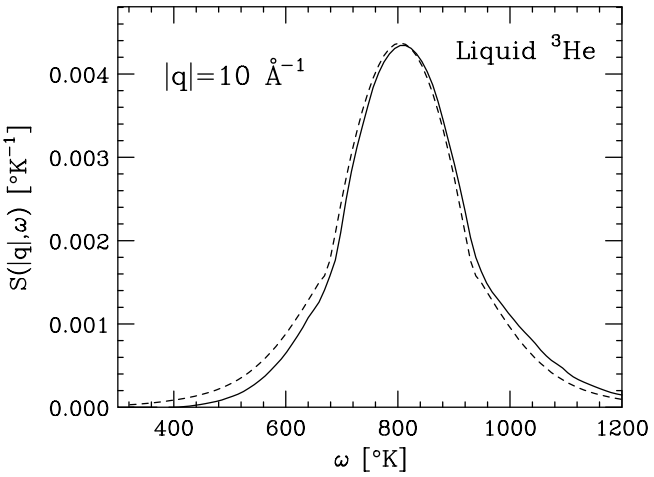

FIG. 2. $S(|\mathbf{q}|, \omega)$ in liquid ^{3}He at $|\mathbf{q}| = 10$ Å^{-1} and equilibrium density. The solid and dashed lines have been obtained using Eqs. (12) and (19), respectively.

scattering data extends to extremely high $|\mathbf{q}|$, typical values being larger than 10 Å^{-1} and (ii) the analysis has been focused on the region of the peak.

In liquid ^{3}He at equilibrium density ($\rho = 0.016\,35$ Å^{-3}) the half-width of the peak of the response at $|\mathbf{q}| = 10$ Å^{-1} is roughly given by (M denotes the mass of the helium atom) $|\mathbf{q}|k_F/M \sim 200$ K, to be compared to a Fermi energy $\epsilon_F = 2.47$ K, and the shift in ω of $\sim$10 K produced by the removal energy of the struck particle reduces to a very small effect.

The nuclear matter response of Fig. 1, on the other hand, has a half-width of $\sim$250 MeV, to be compared to a Fermi energy $\epsilon_F = 16$ MeV and an average removal energy $\bar{\epsilon} = 61.9$ MeV. As a consequence, the shift between the solid and dashed lines is clearly visible [8]. To observe a comparable effect in liquid ^{3}He, one should consider the response at $|\mathbf{q}| \sim 3$ Å^{-1}, where the half-width of the peak shrinks to $\sim$50 K.

The small effect of the removal energy on the position of the peak of the response of liquid ^{3}He at $\rho = 0.016\,35$ Å^{-3} and $|\mathbf{q}| = 10$ Å^{-1} is illustrated in Fig. 2, where the solid and dashed lines correspond to $S(\mathbf{q}, \omega)$ evaluated from Eqs. (12) and (19), respectively. The momentum distribution and spectral function employed in the calculations have been consistently obtained within the Fermi hypernetted chain formalism and the diffusion Monte Carlo method [9].

In conclusion, we have shown that the two different prescriptions used in the literature to evaluate the response of strongly interacting many-fermion systems correspond to different implementations of the assumptions underlying IA. While minimal use of these assumptions leads to the definition in terms of the spectral function, which correctly takes into account the removal energy distribution of the struck particle, the response obtained from the momentum distribution *does not* include all interaction effects. The excellent agreement between the theoretical $S(\mathbf{q}, \omega)$ obtained from Eq. (19) and the experimental data for liquid ^{3}He at $|\mathbf{q}| \geq 10$ Å^{-1} [9] indicates that this feature is not critical to the analysis of the response of nonrelativistic systems at very large momentum transfer, corresponding to $(|\mathbf{q}|/k_F) > 10$, in the region of the peak. On the other hand, disregarding the removal energy distribution in the calculation of the nuclear matter response at $|\mathbf{q}| \sim 5$ fm^{-1}, corresponding to $(|\mathbf{q}|/k_F) \sim 4$, produces a sizable shift of the quasielastic peak. In addition, away from the peak large discrepancies between the $S(\mathbf{q}, \omega)$ obtained from Eqs. (12) and (19) persist even at very large $|\mathbf{q}|$. Hence, a quantitative study of FSI effects, which are known to be important in the low energy region $\omega \ll |\mathbf{q}|^2/2m$, requires as starting point the IA response calculated using the spectral function.

[1] O. Benhar, A. Fabrocini, and S. Fantoni, Nucl. Phys. **A505**, 267 (1989).
[2] C. Carraro and S. E. Koonin, Phys. Rev. B **41**, 6741 (1990).
[3] O. Benhar, A. Fabrocini, S. Fantoni, G. A. Miller, V. R. Pandharipande, and I. Sick, Phys. Rev. C **44**, 2328 (1991).
[4] D. B. Day, J. S. McCarthy, T. W. Donnelly, and I. Sick, Annu. Rev. Nucl. Part. Sci. **40**, 357 (1990).
[5] At $|\mathbf{q}| = 5$ fm^{-1} the ratio $|\mathbf{q}|/m_N$, m_N being the nucleon mass, is $\sim$1, and relativistic kinematics should be used in the calculation of $S(\mathbf{q}, \omega)$. However, the conclusions of the present discussion are unaffected by the nonrelativistic approximation employed to obtain the curves shown in Fig. 1.
[6] O. Benhar, A. Fabrocini, S. Fantoni, and I. Sick, Nucl. Phys. **A579**, 493 (1994).
[7] T. R. Sosnick, W. M. Snow, R. N. Silver, and P. E. Sokol, Phys. Rev. B **43**, 216 (1991).
[8] Note that when relativistic kinematics is used in the calculation of the nuclear matter response, the half-width of the peak at $|\mathbf{q}| \geq 5$ fm^{-1} reduces to $\sim$125 MeV, independent of $|\mathbf{q}|$, and the energy shift displayed in Fig. 1 becomes even more visible.
[9] S. Moroni, S. Fantoni, and A. Fabrocini, Phys. Rev. B **58**, 11 607 (1998).